

Energy Spectra of Few-Electron Quantum Dots

E Anisimovas[†] § and A Matulis[‡] ||

[†] Vilnius University, Sauletekio 9, 2054 Vilnius, Lithuania

[‡] Semiconductor Physics Institute, Gostauto 11, 2600 Vilnius, Lithuania

Abstract. We present the renormalized perturbation series for the energy spectrum of the parabolic quantum dot with 2 – 5 electrons considering ground and the lowest excited states. The proper classification of asymptotic energy levels is performed and behaviour of energy levels from quantum to semiclassical regime is traced. Comparison between the present results and those of exact numerical Hamiltonian diagonalization shows a fair accuracy of the proposed method over the whole range of the electron-electron coupling constant and magnetic field values. The obtained results indicate that increasing of the number of electrons in a dot leads to more classic behaviour of the system.

PACS numbers: 71.10.+x; 73.20.Dx; 03.65.-w

Short title: Energy Spectra of Few-Electron Quantum Dots

July 21, 2021

§ Present address: Department of Theoretical Physics, University of Lund, Sölvegatan 14A, S-223 62 Lund, Sweden.

|| Electronic mail: matulis@uj.pfi.lt

1. Introduction

Quantum dots have been studied extensively as low-dimension nanostructures interesting from the intrinsic theoretical point of view and due to their importance to modern electronic devices [1]. The most spectroscopy experiments were carried out on quantum dots with soft parabolic confinement potential [2]. Those parabolic quantum dots attract the attention as simple model systems for electron-electron interaction studies. Although the parabolic quantum dots have some disadvantage due to Kohn theorem [3] which shows that only the center of mass motion usually can be excited (in absorption and even in tunneling), the confining potential in a dot very often is rather close to the parabolic one. That is why the parabolic dots can serve as a good starting point or the reference for the investigations of more sophisticated quantum dots. The small nonparabolicity usually helps to reveal peculiarities of the relative electron motion spectrum which is sensitive to the electron-electron interaction.

Only in the case of quantum dot with two electrons the exact analytical solution of the eigenvalue problem for the parabolic dot can be obtained [4]. The most of theoretical investigations were mainly based either on some mathematical tricks (which is possible in the case of parabolic dot with 2 and 3 electrons [5, 6]), or on the straightforward diagonalization of the Coulomb interaction [7]. Although the latter gives the exact solution of the problem, due to time consuming calculations it can be applied only in the case of small number of electrons in a dot. That is why the construction of approximate solutions is of interest. One of them was demonstrated in [8] where in the case of high magnetic field rather accurate results were obtained using the moving Eckardt frame. Recently it was shown [9] that some approximate technique based on the renormalized perturbation series can be successfully used for the energy spectrum estimations in a wide coupling constant range. The other technique based on Pade approximants [10] was shown to be very successful in the case of parabolic dot with small number of electrons. Both of those approximations are based on some interpolating technique between the perturbation series in coupling constant and the asymptotic expansion valid in large coupling constant range.

In the present paper in order to obtain the total picture of energy spectrum, including the ground and some excited states, we performed the proper classification of the asymptotic energy levels paying attention to the symmetry properties of the spin wave function part and constructed the renormalized perturbation series for the energy of quantum dots with 2 – 5 electrons based on rather simple two term expansion in both limiting regions of the coupling constant.

The present paper is organized as follows. In section 2 the problem is formulated and the perturbation series technique is outlined. The asymptotic series are formulated in section 3 and the spin wave function part for asymptotic region is constructed in section

4. The interpolating technique is described in section 5 and in the last section 6 the results for quantum dots with 2 – 5 electrons are presented and discussed. In appendix A the algebraic expression for Coulomb matrix element is given and in appendix B all coefficients which are necessary for construction of the renormalized perturbation series are collected.

2. Perturbation series

Generally the system of N electrons in a quasi-2D quantum dot is described by the following Hamiltonian

$$H = \sum_{i=1}^N \left[-\frac{\hbar^2}{2m} \nabla_i^2 + \frac{m\omega_0^2}{2} \mathbf{r}_i^2 \right] + \sum_{i<j}^N \frac{e^2}{\epsilon |\mathbf{r}_i - \mathbf{r}_j|}. \quad (1)$$

Here m stands for the effective electron mass, ϵ is the static dielectric constant, and ω_0 is the characteristic frequency of parabolic confinement potential. For the sake of convenience we shall scale the coordinates $\mathbf{r} \rightarrow a_0 \mathbf{r}$ ($a_0 = \sqrt{\hbar/m\omega_0}$) and measure the energies in dimensionless units of $\hbar\omega_0$. After this transformation we obtain the dimensionless Hamiltonian

$$H = \frac{1}{2} \sum_{i=1}^N (-\nabla_i^2 + \mathbf{r}_i^2) + \lambda \sum_{i<j}^N \frac{1}{|\mathbf{r}_i - \mathbf{r}_j|} = H_0 + \lambda V \quad (2)$$

with the single dimensionless coupling constant $\lambda = a_0/a_B$ ($a_B = \epsilon\hbar^2/me^2$ is the effective Bohr radius) characterizing the energy spectrum of electrons in the parabolic quantum dot.

The simplest way to solve the eigenvalue problem is just to use the perturbation series in coupling constant λ

$$E(\lambda) = E_0 + E_1\lambda. \quad (3)$$

The first coefficient is the eigenvalue of the unperturbed Hamiltonian H_0 and can be presented as the sum of noninteracting electron energies

$$E_0 = \sum_{i=1}^N \varepsilon(i), \quad \varepsilon(i) = 1 + |m_i| + 2n_i \quad (4)$$

where $i = (n_i, m_i, s_i)$ labels the one electron quantum number set.

The first order correction E_1 can be estimated in a standard way (see, for instance [11]) and presented as a sum of two-electron Coulomb matrix elements

$$\langle ij|V|j'i' \rangle = \delta_{s_i, s_{i'}} \delta_{s_j, s_{j'}} \int d^2r_1 \int d^2r_2 \frac{1}{|\mathbf{r}_i - \mathbf{r}_j|} \phi^*(i|\mathbf{r}_1) \phi^*(j|\mathbf{r}_2) \phi(j'|\mathbf{r}_2) \phi(i'|\mathbf{r}_1) \quad (5)$$

where the one electron wave functions can be expressed in associated Laguerre polynomials

$$\phi(n, m|r, \varphi) = \sqrt{\frac{2n!}{2\pi(|m| + n)!}} e^{im\varphi} r^{|m|} e^{-r^2/2} L_n^{|m|}(r^2). \quad (6)$$

For numerical estimation of the Coulomb matrix element (5) we used the analogue of Girvin and Jach expression [12] which is given in Appendix A.

When calculating the first order correction the main problem is the degeneracy of zero order energy levels because the good quantum numbers of the total angular momentum M and the total spin S are not sufficient for classification of energy levels. That is why we used numerical diagonalization of the degenerate blocks of the above first order correction matrix. The obtained results – the coefficients E_0 and E_1 are collected in Appendix B.

3. Asymptotic expansion

In the $\lambda \rightarrow \infty$ case the kinetic energy of the electron system is small if compared to the potential one. It is known that such systems are strongly correlated and show tendency for Wigner crystallization [13]. Monte Carlo results for classical particles in the parabolic dot [14] show that the particles crystallize in some structure of concentric rings. When the number of electrons in a dot is small $N \leq 5$ they fall into a single ring on which the electrons are located equidistantly and separated by the angle $\alpha = 2\pi/N$. The quantum dynamics of such a Wigner crystal can be described by means of the rotation and vibration modes. The general theory of vibration modes is given in [8]. It is based on introducing the moving Eckardt frame and the diagonalization of the vibrational Hamiltonian in the harmonic approach. In the case of small number of electrons located on a single ring the vibrational Hamiltonian and the problem of its diagonalization can be essentially simplified by representing the electron coordinates as complex variables $z = x + iy$ and turning them to the local electron coordinates on the ring by means the following transformation

$$z_n \rightarrow (R + z_n)e^{i\alpha n}. \quad (7)$$

Here n labels the electrons on the ring. We shall follow the simpler way restricting our consideration by the following two term asymptotic expansion

$$E(\lambda) = c_0\lambda^{2/3} + c_1. \quad (8)$$

The first term of it can be easily obtained minimizing the potential in (2). The minimization leads to the equilibrium ring radius $R = (\lambda A)^{1/3}$ (where $A = \sum_{n=1}^{N-1} |4 \sin(\alpha n/2)|^{-1}$) which corresponds to the main term $c_0\lambda^{2/3} = 1.5NR^2$ in the

asymptotic energy expansion. The next term in expansion (8) corresponds to the ring oscillations. To obtain it we insert (7) into Hamiltonian (2) and expand the potential into z -series. It leads to the following second order correction to the equilibrium potential

$$V_2 = \frac{1}{2} \sum_{n=1}^N |z_n|^2 + \frac{N}{32A} \sum_{n=1}^{N-1} (3\gamma_n^2 + 3\gamma_n^{*2} + 2|\gamma_n|^2)$$

where

$$\gamma_{nm} = \frac{z_n e^{i\alpha n} - z_m e^{i\alpha m}}{e^{i\alpha n} - e^{i\alpha m}} = \frac{z_n [1 - e^{i\alpha(n-m)}] + z_m [1 - e^{i\alpha(m-n)}]}{4 \sin^2[\alpha(n-m)/2]} \equiv \gamma_{n-m}.$$

Now let us apply the Fourier transform

$$z_n = \frac{1}{\sqrt{N}} \sum_k e^{ik\alpha n} z_k \quad (9)$$

where $k = 0, 1, \dots, N-1$ denotes the vibration modes. Inserting it into the above potential expression and subsequently into (2) after simple but laborious transformation we obtain the following expression for the asymptotic Hamiltonian with the second order potential corrections

$$H = \sum_k H_k = \sum_k \left\{ -2 \frac{\partial^2}{\partial z_k \partial z_k^*} + A_k z_k z_k^* + B_k (z_k z_{-k} + z_k^* z_{-k}^*) \right\} \quad (10)$$

where

$$A_k = \frac{1}{2} + \frac{1}{16A} \sum_{n=1}^{N-1} |\sin(\alpha n/2)|^{-3} \sin^2[(k+1)\alpha n/2],$$

$$B_k = \frac{3}{32A} \sum_{n=1}^{N-1} |\sin(\alpha n/2)|^{-3} [\sin^2(\alpha n/2) - \sin^2(k\alpha n/2)].$$

The Hamiltonian is composed of parts H_k which describe the behaviour of both polarization of $\pm k$ modes as a system of four coupled harmonic oscillators. They can be diagonalized in a standard way just introducing the proper variables. Let us separate the real and imaginary parts of the initial variables, and introduce the new variables in the following way

$$z_k = x + iy, \quad z_{-k} = u + iv. \quad (11)$$

In these variables every Hamiltonian (10) part H_k splits into two terms. The first term is

$$H_k^{(1)} = -\frac{1}{2} \left(\frac{\partial^2}{\partial x^2} + \frac{\partial^2}{\partial u^2} \right) + A_k x^2 + A_{-k} u^2 + 2(B_k + B_{-k})xu \quad (12)$$

while the other part $H_k^{(2)}$ can be obtained just replacing $x \rightarrow y$ and $u \rightarrow -v$.

Both $H_k^{(1,2)}$ have the same eigenvalues that can be found by the diagonalization of the symmetric matrix

$$\begin{pmatrix} A_k & B_k + B_{-k} \\ B_k + B_{-k} & A_{-k} \end{pmatrix}$$

which defines the quadratic form of the potential term, and leads to the following expression for the eigenfrequencies

$$\omega_k^{(\pm)} = \sqrt{A_k + A_{-k} \pm \sqrt{[A_k - A_{-k}]^2 + 4[B_k + B_{-k}]^2}}. \quad (13)$$

Thus, since the transformed Hamiltonian corresponds to the set of independent harmonic oscillators the corresponding vibration wave function Φ can be constructed in a standard way introducing the ‘‘phonon’’ creation $a_{k,\beta}^\dagger$ and annihilation $a_{k,\beta}$ operators

$$\Phi = a_{k_1,\beta_1}^\dagger \cdots a_{k_p,\beta_p}^\dagger |0\rangle. \quad (14)$$

The ‘‘vacuum’’ state $|0\rangle$ corresponds to the system ground state, and the symbol $\beta = 1, 2$ stands for polarization.

For the interpolation purposes it is important to know the wave function symmetry properties with respect to the rotation of the electronic ring as a whole. Let us denote this operation by operator \mathcal{P} . It is evident that the ground state is invariant under that operation, i. e. $\mathcal{P}|0\rangle = |0\rangle$. As the above rotation is equivalent to the substitution $n \rightarrow n + 1$ it follows from expression (9) that $\mathcal{P}z_k = \exp(ik)z_k$. Due to the mixing of both $\pm k$ modes the operators $a_{k,\beta}^\dagger$ and wave function (14) obey more complicated symmetry condition. However, because of the degeneracy of obtained vibration states it can be essentially simplified using the proper superposition of the eigenstates of both Hamiltonian parts $H_k^{(1,2)}$. So, we shall assume that the wave function superposition of this sort is constructed, and consequently the phonon operators obey the symmetry condition

$$\mathcal{P}a_{k,\alpha}^\dagger = e^{-ik} a_{k,\alpha}^\dagger. \quad (15)$$

We shall use the above symmetry condition for the classification of obtained asymptotic vibration modes whose frequencies $\omega_k^{(\beta)}$ are collected in table 1. Two modes with eigenfrequencies $\omega_k^{(\beta)} = 1$ correspond to the center of mass motion. We do not take them into account as we consider the electron relative motion energy spectrum only. The mode $k = 0$ corresponds to the ‘breathing’ mode for $\beta = 1$ and to the rotation of the ring as a whole for $\beta = 2$. The last case should be considered separately. Actually, in the harmonic approximation used the rotation mode is separated from the vibration modes. Its eigenfunction is $\exp(iM\varphi)$ (φ is an angle determining rotation of the ring as a whole) and the corresponding energy is $M^2/2NR^2 \sim \lambda^{-2/3}$. It is seen that in the case of large angular momenta M this term becomes essential and thus it should be included into the

Table 1. The ring vibration frequencies and the asymptotic expansion coefficients

N	2		3		4		5		
k	β	1	2	1	2	1	2	1	2
0		1.7321	0.0	1.7321	0.0	1.7321	0.0	1.7321	0.0
1		1.0	1.0	1.2247	1.0	1.3186	1.0	1.3719	1.0
2				1.2247	1.0	1.4888	0.8852	1.6890	0.7274
3						1.3186	1.0	1.6890	0.7274
4								1.3719	1.0
	c_0	1.1905		3.1201		5.8272		9.2801	
	$c_1^{(0)}$	1.8660		3.0908		4.3716		5.6544	

main asymptotic energy term, and consequently it leads to the equilibrium ring radius dependence on the total angular momentum M (see [8] for instance). However, the above term is of order $\lambda^{-2/3}$ and lies beyond the (8) approximation. Hence considering the states with small M only we neglect this rotation mode correction (and the ring radius dependence on M as well) together with the anharmonicity corrections which are of the same order of magnitude. We should keep in mind, however, that there are many states labeled by different M values corresponding to every asymptotic vibration term.

Thus, the first order correction is given by

$$c_1 = c_1^{(0)} + \sum_{k,\beta} n_{k,\beta} \omega_k^{(\beta)}$$

where $c_1^{(0)}$ is the contribution of the ground vibration state energy and the symbol $n_{k,\beta}$ stands for the filling factor of the corresponding phonon mode. Those coefficients together with first term coefficients c_0 are given in the last two lines of table 1.

Separating the rotation mode we shall represent the total wave function in the asymptotic region as a product of rotation, vibration and spin parts

$$\Psi = e^{iM\varphi} \Phi \Upsilon. \quad (16)$$

According to the Pauli's principle the total wave function should be antisymmetric. In the asymptotic region the classical electron equilibrium positions are separated by high potential barriers. That is why we shall restrict ourselves only to the physically important permutation — the rotation \mathcal{P} . As the rotation corresponds to the odd permutation in the case of the even number of electrons (and vice versa) the total wave function obeys the following symmetry condition

$$\mathcal{P}\Psi = (-1)^{N-1}\Psi. \quad (17)$$

According to (14–16) the rotation and vibration parts obey the condition

$$\mathcal{P}e^{iM\varphi}\Phi = e^{i\alpha(M-\gamma)}e^{iM\varphi}\Phi, \quad \gamma = \sum'_{k,\beta} kn_{k,\beta}. \quad (18)$$

The prime in summation indicates that the mode corresponding to the ring rotation is excluded. The different factors in the two above conditions should be compensated by the proper choice of the spin function part.

4. Spin wave function part

Following [8] we diagonalize the \mathcal{P} operator in the S_z (total spin z -projection operator) eigenfunction space and construct the spin function part obeying the symmetry condition

$$\mathcal{P}\Upsilon = e^{i\alpha\tau}\Upsilon \quad (19)$$

which together with (17), (18) leads to the following selection rule

$$M + \tau - \gamma = Np. \quad (20)$$

In the case of odd number N of electrons in a dot the symbol p stands for an arbitrary integer while in the case of the even N it should be replaced by $p + 1/2$. The integer parameter τ which characterizes the spin function part symmetry properties should be defined for every particular case. In the case when the above procedure leads to the degeneracy of spin states the total spin operator S^2 should be diagonalized additionally.

The case of 2 electrons is a trivial one. There is the triplet function $|\uparrow\uparrow\rangle$ with $S_z = 1$ corresponding to $\tau = 0$ and the singlet function $\{|\uparrow\downarrow\rangle - |\downarrow\uparrow\rangle\}/\sqrt{2}$ with $S_z = 0$ corresponding to $\tau = 1$. We shall not consider the functions with $S_z < 0$ as they give no extra information.

The case of 3 electrons is considered in detail in [8]. There is quartet state corresponding to $\tau = 0$ and two doublet states with $\tau = \pm 1$.

Applying the same treatment to the system with 4 and 5 electrons we obtain the spin function parts with the symmetry properties of (19) type. All the necessary τ values are collected in table 2.

The above selection rule gives us the possible terms for every vibration state characterized by γ value. The terms for the ground vibration state ($\gamma = 0$) are collected in the last column of table 2. For the sake of brevity we use the notation analogous to that adopted in atomic spectroscopy. Thus the capital letters S, P, D, \dots indicate the corresponding $M = 0, 1, 2, \dots$ values, and the left superscript symbol stands for multiplicity $(2S+1)$. The terms corresponding to the excited vibration states with $\gamma \neq 0$ can be easily obtained from those presented in table 2 applying the shift $M \rightarrow M + \gamma$. Further we shall label those excited terms with the additional right underscript symbol k indicating the modes of the phonons present in that state.

Table 2. τ values for the various multiplets and the ground state terms.

N	$S = 0$	$S = 1/2$	$S = 1$	$S = 3/2$	$S = 2$	$S = 5/2$	Terms
2	1	-	0	-	-	-	$^1S, ^3P, ^1D, ^3F, \dots$
3	-	1,2	-	0	-	-	$^4S, ^2P, ^2D, ^4F, \dots$
4	0,2	-	1,2,3	-	0	-	$^{1,3}S, ^3P, ^{1,5}D, ^3F, ^{1,3}G, \dots$
5	-	0,1,2,3,4	-	1,2,3,4	-	0	$^{2,6}S, ^{2,4}P, ^{2,4}D, ^{2,4}F, ^{2,4}G \dots$

5. Interpolation

In constructing the interpolating expression we shall follow [9] where the perturbation series renormalization procedure is given in details. The main idea is replacing of (2) by the generalized Hamiltonian

$$H = \frac{1}{2} \sum_{i=1}^N (-\xi^2 \nabla_i^2 + \mathbf{r}_i^2) + \lambda \sum_{i < j} \frac{1}{|\mathbf{r}_i - \mathbf{r}_j|}, \quad (21)$$

and using the scaling relation for the generalized eigenvalue

$$E(\xi, \lambda) = \xi E(1, \lambda \xi^{-3/2}). \quad (22)$$

The eigenvalue of the basic problem with Hamiltonian (2) is given as $E(\lambda) = E(1, \lambda)$.

The scaling relation defines the trajectory $\lambda = \lambda_0 \xi^{3/2}$ in the $\xi\lambda$ -plane as it is shown in figure A1. That trajectory enables to map the vertical dashed line $\xi = 1$ (where we need to obtain the eigenvalue of the basic problem) onto tilted line KP which we define as

$$\begin{aligned} \lambda &= K\beta, & K &= (1 + \tan \phi)/2 \\ \xi &= P(1 - \beta), & P &= (1 + \cot \phi)/2. \end{aligned} \quad (23)$$

For instance, the point λ_0 is mapped to the point (ξ, λ) .

Contrary to line $\xi = 1$ the line KP is located in the finite region of the $\xi\lambda$ -plane ($0 < \beta < 1$), and that is why the energy $E(\xi(\beta), \lambda(\beta))$ can be successfully expanded into β -series. Adjusting the above series to the λ -series (3) in the region $\lambda \rightarrow 0$ and to the asymptotic expansion (8) in the region $\lambda \rightarrow \infty$ we obtain the final expression for the renormalized series

$$\begin{aligned} E &= (b_0 + b_1\beta + b_2\beta^2 + b_3\beta^3)/(1 - \beta) \\ \lambda &= \frac{K\beta}{P^{3/2}(1 - \beta)^{3/2}}. \end{aligned} \quad (24)$$

The expansion coefficients can be expressed in terms of those in (3) and (8) as

$$b_0 = E_0$$

$$\begin{aligned}
b_1 &= KP^{-3/2}E_1 - E_0 \\
b_2 &= 7/3 K^{2/3}P^{-1}c_0 + c_1 - E_0 - 2KP^{-3/2}E_1 \\
b_3 &= -4/3 K^{2/3}P^{-1}c_0 - c_1 + E_0 + KP^{-3/2}E_1.
\end{aligned} \tag{25}$$

As we restricted ourselves with the two term approximation in both (3) and (8) expansions we introduced the additional adjustable parameter ϕ (as proposed in [15]) for improving the interpolating accuracy. The geometric meaning of that parameter is clear from figure A1 — it indicates the rotation angle of the mapping line KP around the point M to which the energy $E(\sqrt{2})$ is always mapped. The rotation changes the relative contributions of the λ -series and the asymptotic expansion to the renormalized series. The value $\phi = 0$ corresponds to the full control of the renormalization procedure by the λ -series and the value $\phi = \pi/2$ to that of the asymptotic expansion.

It was shown in [15] that usually the energy exhibits some plateau as a function of the parameter controlling the mapping line (ϕ in our case). When the number of terms in the λ -series is increased that plateau shows the tendency to increase, too, thus giving a good reason for the controlling parameter choice. In figure A2 the energy at the fixed point $\lambda = \sqrt{2}$ as a function of the parameter ϕ is shown by the solid line in the case of the first excited triplet state of the two electron system. As our λ -series are rather short we have no prominent plateau. However, some curve twist is present, and we hope that it is a rather good idea to choose the controlling parameter ϕ somewhere between the Max and Min points. The difference of energy values corresponding to those points can serve as an estimation of the interpolation accuracy. We see that the accuracy is of about 1%.

We used the inflection point of $E(\sqrt{2})$ versus ϕ curve for the controlling parameter ϕ choice. The energy value obtained with that choice is shown by dashed line in figure A2. Comparing it with the exact result which is known for two electron case (dotted line) we see that the accuracy is even better than 1%. The same energy versus ϕ behaviour and the same accuracy was obtained for all other considered terms. The inflection point values of ϕ for all the considered terms are given in Appendix B in tables A1 and A2. They together with coefficients E_0 , E_1 and expressions (23–25) define the renormalized perturbation series and enable to obtain the energies in the whole range of λ values.

We should note that according to [9] the same parameter values can be used for constructing the renormalized series in the case when the additional magnetic field B is applied in the direction perpendicular to the quantum dot plane. In that case we have

$$E(\lambda, B) = \sqrt{1 + (\omega_c/2\omega_0)^2}E(\lambda') + M\omega_c/2\omega_0 + g^*\mu_B B S_z/\hbar\omega_0 \tag{26}$$

and

$$\lambda' = \lambda[1 + (\omega_c/2\omega_0)^2]^{-1/4} \tag{27}$$

where the symbol $\omega_c = eB/mc$ stands for cyclotron frequency. Note that there is a misprint in (5.4) of [9]. The last term added in (26) corresponds to the Zeeman energy where g^* is the effective g factor and μ_B is the Bohr magneton.

6. Results and discussion

As an illustration of the introduced renormalization technique we present in figures A3–A6 the excitation energy versus λ plot for the relative electron motion for the quantum dot with 2–5 electrons. The inclusion of the center of mass motion energy is a trivial one. One should just shift up the presented spectra by the some integer value, as the center of mass motion is not affected by the electron interaction.

The main problem is to decide how the terms in both regions ($\lambda \rightarrow 0$ and $\lambda \rightarrow \infty$) should be interconnected. Taking into account the fact known in quantum mechanics that two terms with the same good quantum numbers never cross each other we used the simplest term connection scheme. Starting from the ground state we connected successively term in the region $\lambda \rightarrow 0$ to the lowest possible unconnected term with the same M and S quantum numbers in the asymptotic region.

In figures A3 and A4 the energy plot for the system of two and three electrons are presented. The terms with the zero energy exceeding the ground state energy by 3 and 2, correspondingly, are depicted. In the case of four and five electrons the energy plots are given in figures A5 and A6. The degeneracy of the states grows rapidly with the number of electrons and thus here we present only the two lowest terms tending to each of asymptotic vibration states. The asymptotic terms in the above figures are labeled by the numbers in parenthesis along right axis which indicate the k values of the phonons present in the state. The phonon state with polarization corresponding to the larger frequency is indicated by prime.

It can clearly be seen how the term structure transforms from that of the weakly interacting quantum system, where the energy levels are governed by filling of noninteracting single electron states to the semiclassical strongly correlated system, where the energy levels correspond to the electronic ring vibration frequencies. Such switching of the dot behaviour can be explained by simple dimensional considerations. Namely, the three terms in Hamiltonian (1) can be estimated as $\hbar^2 N/mR^2$, $m\omega_0^2 R^2 N$ and $e^2 N(N-1)/\epsilon R$. Equating them we define the critical λ value $\lambda^* \sim 1/(N-1)$ where the above mentioned switching occurs. This is in agreement with our energy dependencies. As the dimensionless coupling constant λ is proportional to $a_0 \sim 1/\sqrt{\omega_0}$ the above estimation leads to some condition for confinement potential frequency showing whether the dot behaves like quantum system or the classical one. When the confinement potential is mainly caused by some positive neutralizing charge located on the rather distant gate the increase in confinement potential frequency ω_0 does not exceed N [7].

In that case increasing of the number of electrons in a dot leads to more classical system.

As an illustration of the presented renormalized series technique in the case with magnetic field (according to (26)) we calculated the ground state energies vs. magnetic field for 2 – 5 electrons which are displayed in figures A7 (a)–(d). The curve (a) for two electron system is in good agreement with that presented in [7] (we choose the parameters as in [7] and also include the fictitious gate charge but do not subtract the zero point motion of the center of mass). It is seen from figures A7 (b)–(d) that increasing the number of electrons the structure of the dependencies becomes less resolved and the peaks lose their sharpness. Thus we miss a tiny additional peak in the position marked by an arrow in figure A7 (b) which is present in data of exact diagonalization. Comparing our results with those obtained in [8], say, for $N = 3$, $B = 20$ T, $S = 3/2$, $M = 3$ we obtained ground energy value 77.5 meV and find a good coincidence which proves that the approximate separation of rotation and vibration modes works fairly well for small angular momenta.

Concluding we would like to mention that the parabolic quantum dot due to the softness of the confinement potential is rather favourable object for constructing the interpolating expressions in the contrary to the hard wall dot [17] where the accuracy is much worse.

Acknowledgments

One of us (E. A.) is thankful to Prof. Per Hedegård (Ørsted Laboratory, University of Copenhagen) for useful comments.

References

- [1] Johnson N F 1995 *J. Phys.: Condens. Matter* **7** 965
- [2] Meurer B, Heitmann D and Ploog K 1993 *Phys. Rev. B* **48** 11488
- [3] Maksym P A and Chakraborty T 1990 *Phys. Rev. Lett.* **65** 108
- [4] Taut M 1993 *Phys. Rev. A* **48** 3561
- [5] Merkt U, Huser J and Wagner M 1991 *Phys. Rev. B* **43** 7320
- [6] Pfannkuche D and Ulloa S E 1995 *Phys. Rev. Lett.* **74** 1194
- [7] Hawrylak P 1993 *Phys. Rev. Lett.* **71** 3347
- [8] Maksym P A 1996 *Phys. Rev. B* **53** 10871
- [9] Matulis A and Peeters F M 1994 *J. Phys.: Condens. Matter* **6** 7751
- [10] Gonzalez A *J. Phys.: Condens. Matter* (to be published 1997)
- [11] Fjærestad J O, Matulis A and Chao K A 1997 *Physica Scripta* **T69** 138
- [12] Girvin S M and Jach T 1983 *Phys. Rev. B* **28** 4506
- [13] Maksym P A 1993 *Physica B* **184** 385
- [14] Bedanov V M and Peeters F M 1994 *Phys. Rev. B* **184** 2667
- [15] Fernández F M, Artega G A, Maluendes S A and Castro E 1984 *Phys. Lett.* **103A** 19

[16] Stone M, Wyld H W and Schult R L 1992 *Phys. Rev. B* **45** 14156

[17] Matulis A, Fjærrestad J O and Chao K A *Physica Scripta* 1997 **T69** 85–91

Appendix A. Coulomb matrix element

In [12] the algebraic expression for calculation of the two-particle matrix element of Coulomb interaction of electrons in the lowest Landau level (corresponding to $n_i = 0$ in our case) was used (see the comments in [16]). In more general ($n_i \neq 0$) case the analogous Girvin and Jach expression can be derived employing the same center of mass and relative motion complex coordinate technique after expanding the associated Laguerre polynomials in sums and representing the terms in form

$$(r_1 e^{-i\varphi_1})^{\gamma_1} (r_2 e^{-i\varphi_2})^{\gamma_2} (r_2 e^{i\varphi_2})^{\gamma_3} (r_1 e^{i\varphi_1})^{\gamma_4} \frac{e^{-(r_1^2 + r_2^2)}}{|\mathbf{r}_1 - \mathbf{r}_2|},$$

here the symbols γ_i stand for some numbers

$$\begin{aligned} \gamma_1 &= j_1 + j_4 + (|m_1| + m_1)/2 + (|m_4| - m_4)/2, \\ \gamma_4 &= j_1 + j_4 + (|m_1| - m_1)/2 + (|m_4| + m_4)/2. \end{aligned} \quad (\text{A1})$$

Symbols j_i are integer summation indices running from 0 to n_i . γ_2 and γ_3 can be obtained from (A1) replacing the indices $1 \rightarrow 2$ and $4 \rightarrow 3$. The final expression reads

$$\begin{aligned} \langle 12|V|34 \rangle &= \delta_{s_1, s_4} \delta_{s_2, s_3} \delta_{m_1 + m_2, m_3 + m_4} \left[\prod_{i=1}^4 \frac{n_i!}{(|m_i| + n_i)!} \right]^{1/2} \sum_{(4)j=0}^n \frac{(-1)^{j_1 + j_2 + j_3 + j_4}}{j_1! j_2! j_3! j_4!} \\ &\times \left[\prod_{i=1}^4 \binom{n_i + |m_i|}{n_i - j_i} \right] \frac{1}{2^{(G+1)/2}} \sum_{(4)l=0}^{\gamma} (-1)^{\gamma_2 + \gamma_3 - l_2 - l_3} \\ &\times \delta_{l_1 + l_2, l_3 + l_4} \left[\prod_{i=1}^4 \binom{\gamma_i}{l_i} \right] \Gamma\left(1 + \frac{\Lambda}{2}\right) \Gamma\left(\frac{G - \Lambda + 1}{2}\right) \end{aligned} \quad (\text{A2})$$

where

$$\sum_{(4)j=0}^n \equiv \sum_{j_1=0}^{n_1} \sum_{j_2=0}^{n_2} \sum_{j_3=0}^{n_3} \sum_{j_4=0}^{n_4}, \quad G = \sum_i \gamma_i, \quad \Lambda = \sum_i l_i, \quad \binom{n}{m} = \frac{n!}{m!(n-m)!}.$$

Although the above expression involves terms with alternating signs and leads to numerical difficulties in the case of large quantum number values [16], we found it rather convenient and accurate in the case of quantum dots with small number of electrons.

Appendix B. Expansion coefficients

Here the perturbation series (3) coefficients E_0 and E_1 , and the inflection point angle ϕ are presented for all terms under consideration. Those values together with the

asymptotic expansion (8) given in table 1 and expressions (23–25) are sufficient for constructing the renormalized perturbation series.

Table A1. Coefficients for quantum dot with $N = 2$ and $N = 3$ electrons.

$N = 2$				$N = 3$			
Term	E_0	E_1	ϕ	Term	E_0	E_1	ϕ
1S	2	1.2533	0.3571	2P	4	2.8200	0.5871
3P	3	0.6267	1.2211	4S	5	1.8800	1.0722
1D	4	0.4700	1.3993	2D	5	2.2325	0.9358
1S_0	4	0.9400	0.7204	2S_1	5	2.5850	0.5836
3F	5	0.3917	1.4651	4F	6	1.7037	1.1984
3P_0	5	0.5483	1.3065	4P_1	6	1.8212	1.0783
				2P_1	6	1.8413	1.0698
				2F_1	6	2.2618	0.8991
				2P_0	6	2.5942	0.7067

Table A2. Coefficients for quantum dot with $N = 4$ and $N = 5$ electrons.

$N = 4$				$N = 5$			
Term	E_0	E_1	ϕ	Term	E_0	E_1	ϕ
3S	6	5.0133	0.6105	2P	8	8.3032	0.4913
1D	6	5.2483	0.5800	4D	9	7.4416	0.6649
1S	6	5.4832	0.5527	2S	9	7.4812	0.6607
3P	7	4.3608	0.8333	4S_2	9	7.6765	0.6409
3F	7	4.6412	0.7828	2S_2	9	7.7647	0.6325
1P_1	7	4.6999	0.6087	2G	9	7.8234	0.6270
3P_2	7	4.8628	0.6482	2D	9	7.8284	0.6265
5D	8	3.5641	1.0635	2D_2	9	8.1710	0.5969
5S_2	8	3.6816	0.9920	2S_2	9	8.3125	0.5263
3S_1	8	3.9491	0.8956	4P	10	6.7149	0.8303
1S_2	8	3.9822	0.9218	4F	10	6.8596	0.8110
3D_2	8	4.0215	0.9130	4P_2	10	6.9609	0.7980
1G	8	4.0919	0.9543	2F	10	6.9615	0.7980
3G	8	4.1320	0.9466	2P_2	10	7.1355	0.7768
1D_2	8	4.3311	0.8487	4F_2	10	7.2010	0.7224
3D_1	8	4.3783	0.8004	2P_2	10	7.2489	0.7168
$^1S_{2'}$	8	4.3866	0.7810	2H	10	7.2543	0.7631
3S_1	8	4.5628	0.7656	2F_2	10	7.3103	0.7568
3D_1	8	4.5642	0.7654	4P_2	10	7.3563	0.7046
1G_2	8	4.6678	0.7885	2P_1	10	7.4043	0.6993
$^1D_{2'}$	8	4.7087	0.7220	2P_1	10	7.5375	0.6783
3S_0	8	4.7653	0.6836	2F_2	10	7.6303	0.6757
1S_0	8	4.8182	0.6751	2F_1	10	7.6670	0.6720
1D_0	8	5.0062	0.6472	$^2P_{2,2}$	10	7.9283	0.6407
$^1S_{2,2}$	8	5.2186	0.6140	$^2P_{2,2}$	10	8.0142	0.6331

Figure captions

Figure A1. Mapping in the $\xi\lambda$ -parameter plane.

Figure A2. The first excited triplet state for two electrons: 1, Energy versus ϕ plot; 2, the exact result; 3, energy value at the inflection point.

Figure A3. Spectrum for two electrons.

Figure A4. Spectrum for three electrons.

Figure A5. Spectrum for four electrons.

Figure A6. Spectrum for five electrons.

Figure A7. Ground state energy of quantum dot in magnetic field: (a) - 2 electrons, (b) - 3 electrons, (c) - 4 electrons, (d) - 5 electrons. Single electron ground state energies $E(1)$ are subtracted.

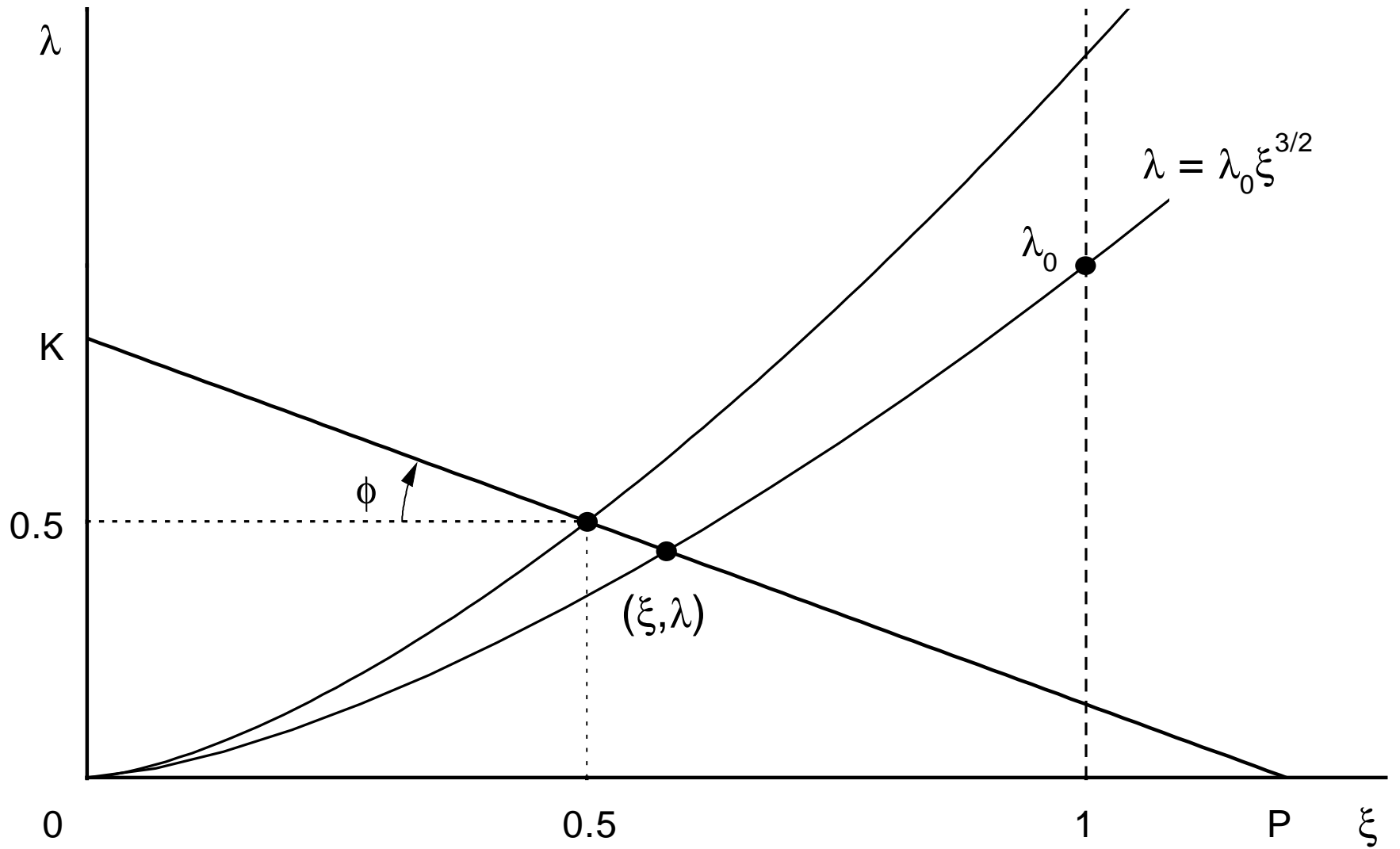


Fig. 1 (E. Anisimovas and A. Matulis "Energy Spectra .

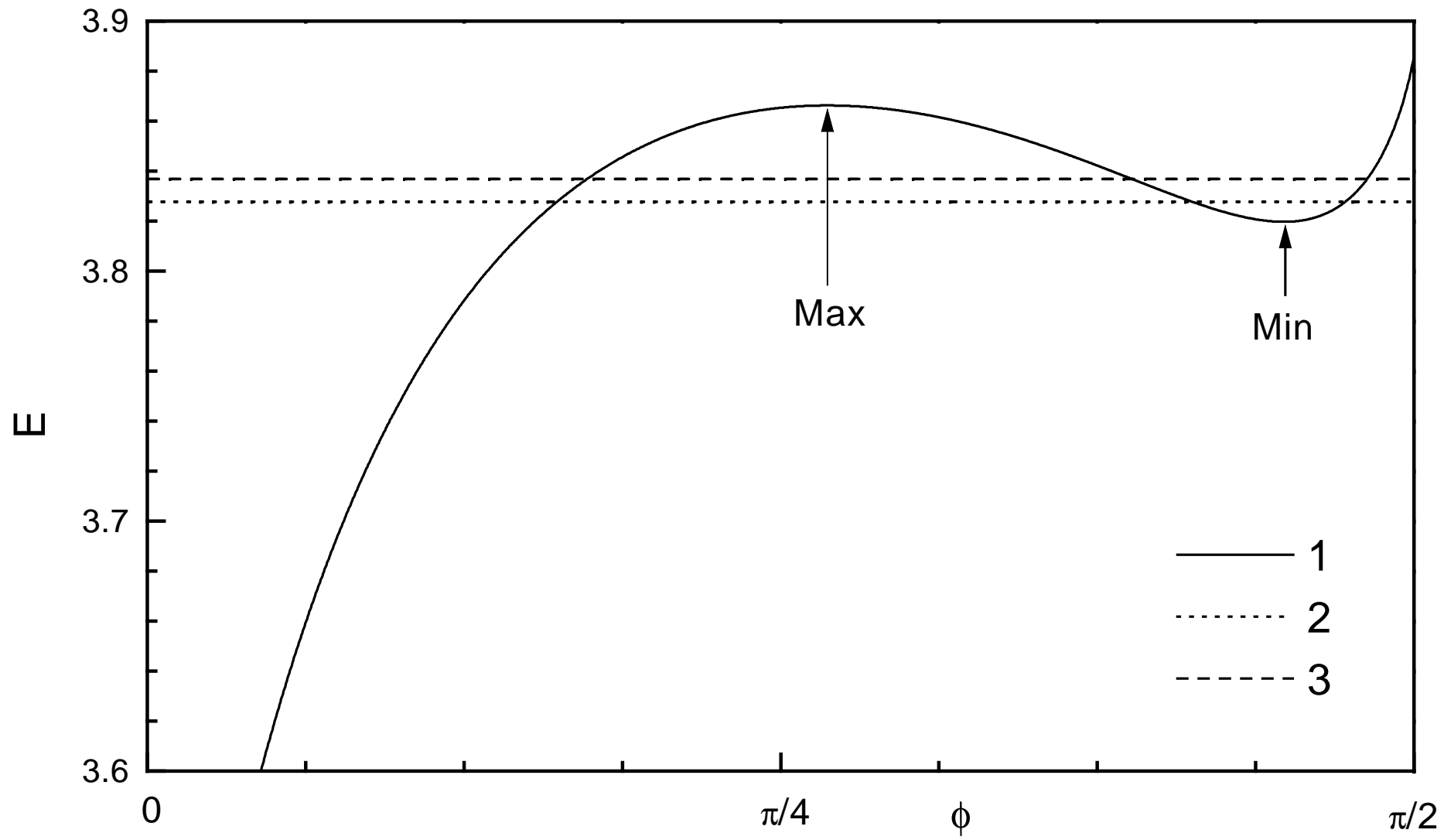


Fig. 2 (E. Anisimovas and A. Matulis "Energy Spectra ...")

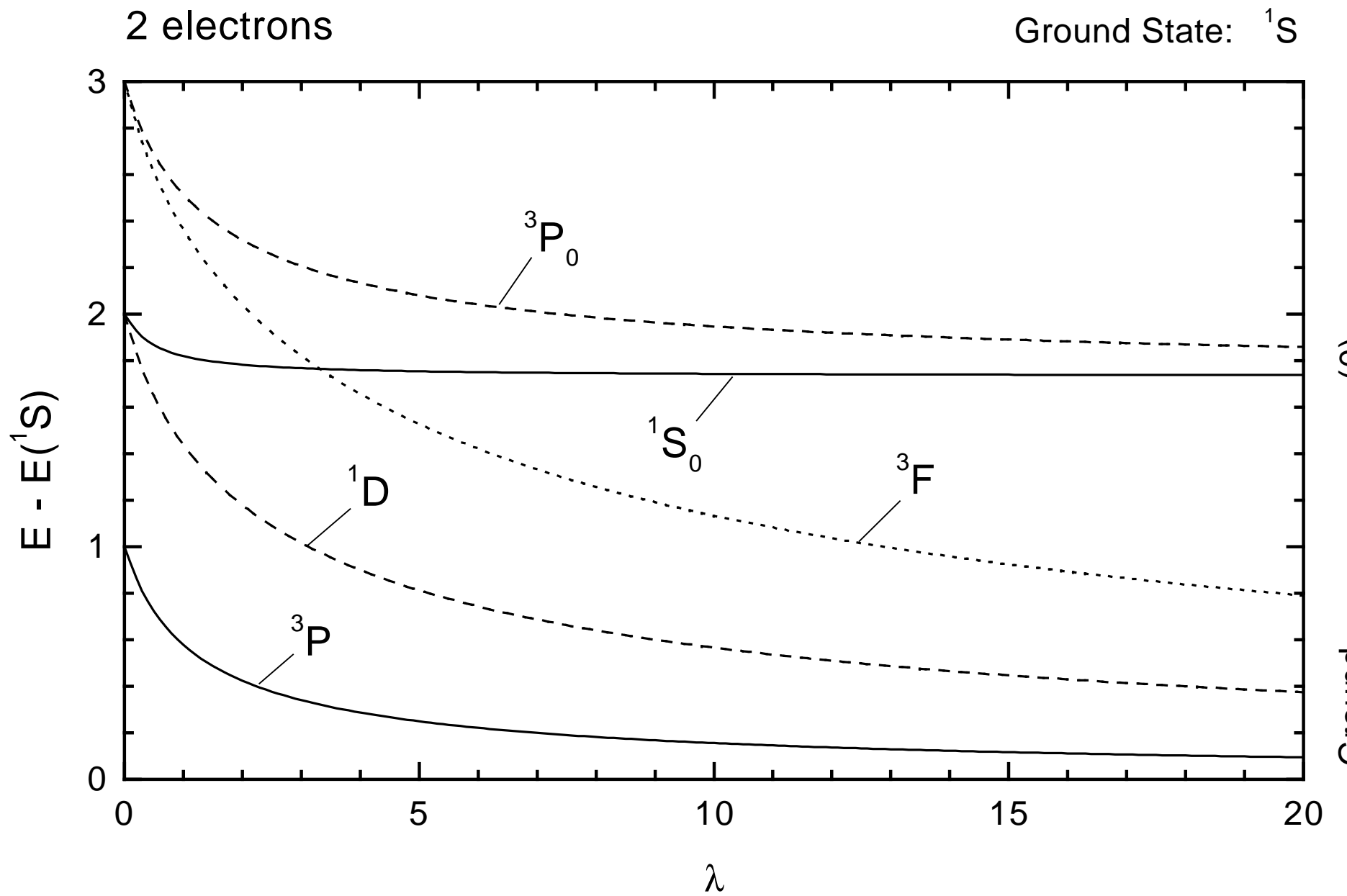


Fig. 3 (E. Anisimovas and A. Matulis "Energy Spectra ... ")

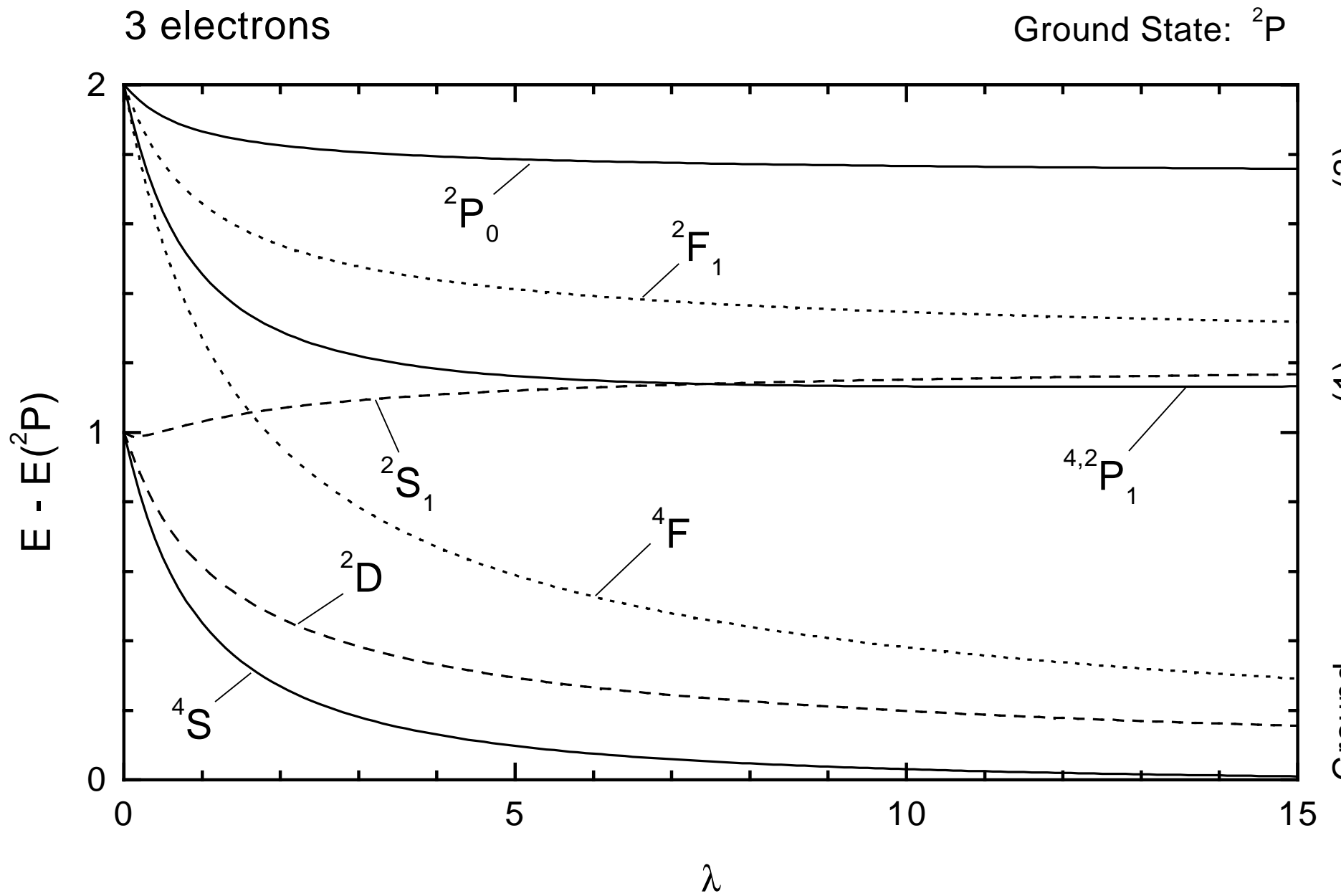


Fig. 4 (E. Anisimovas and A. Matulis "Energy Spectra ... ")

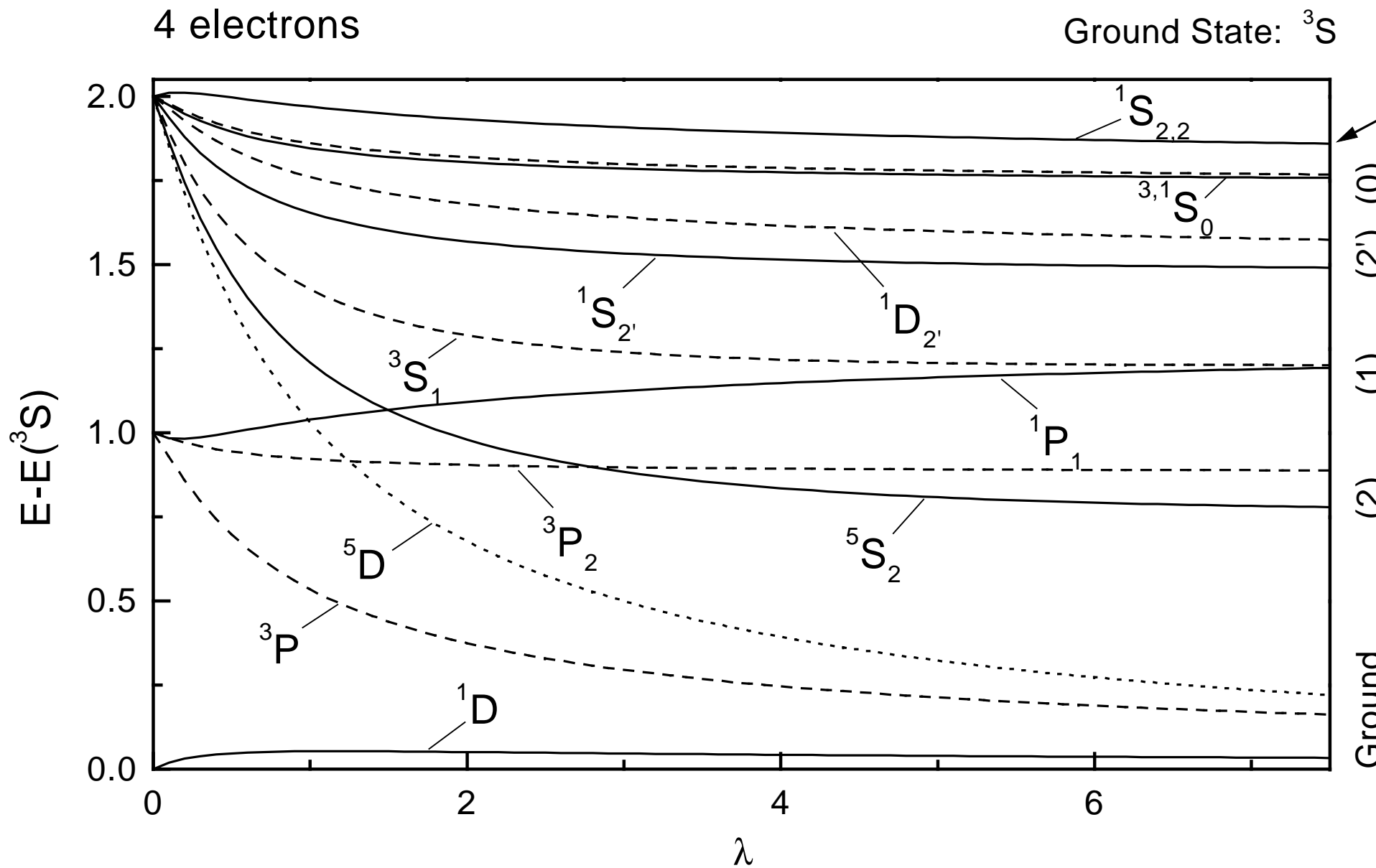


Fig. 5 (E. Anisimovas and A. Matulis "Energy Spectra ... ")

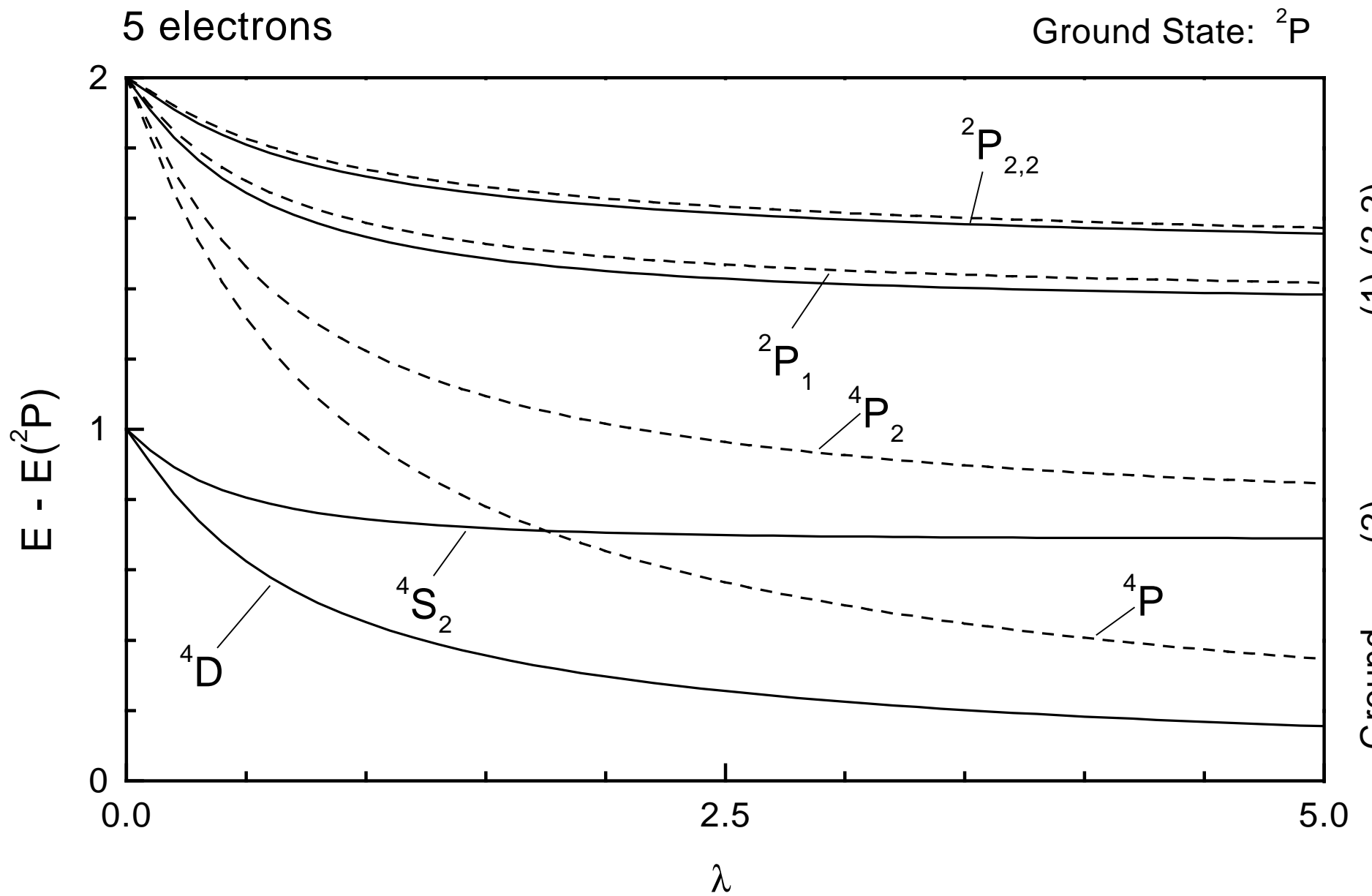


Fig. 6 (E. Anisimovas and A. Matulis "Energy Spectra ... ")

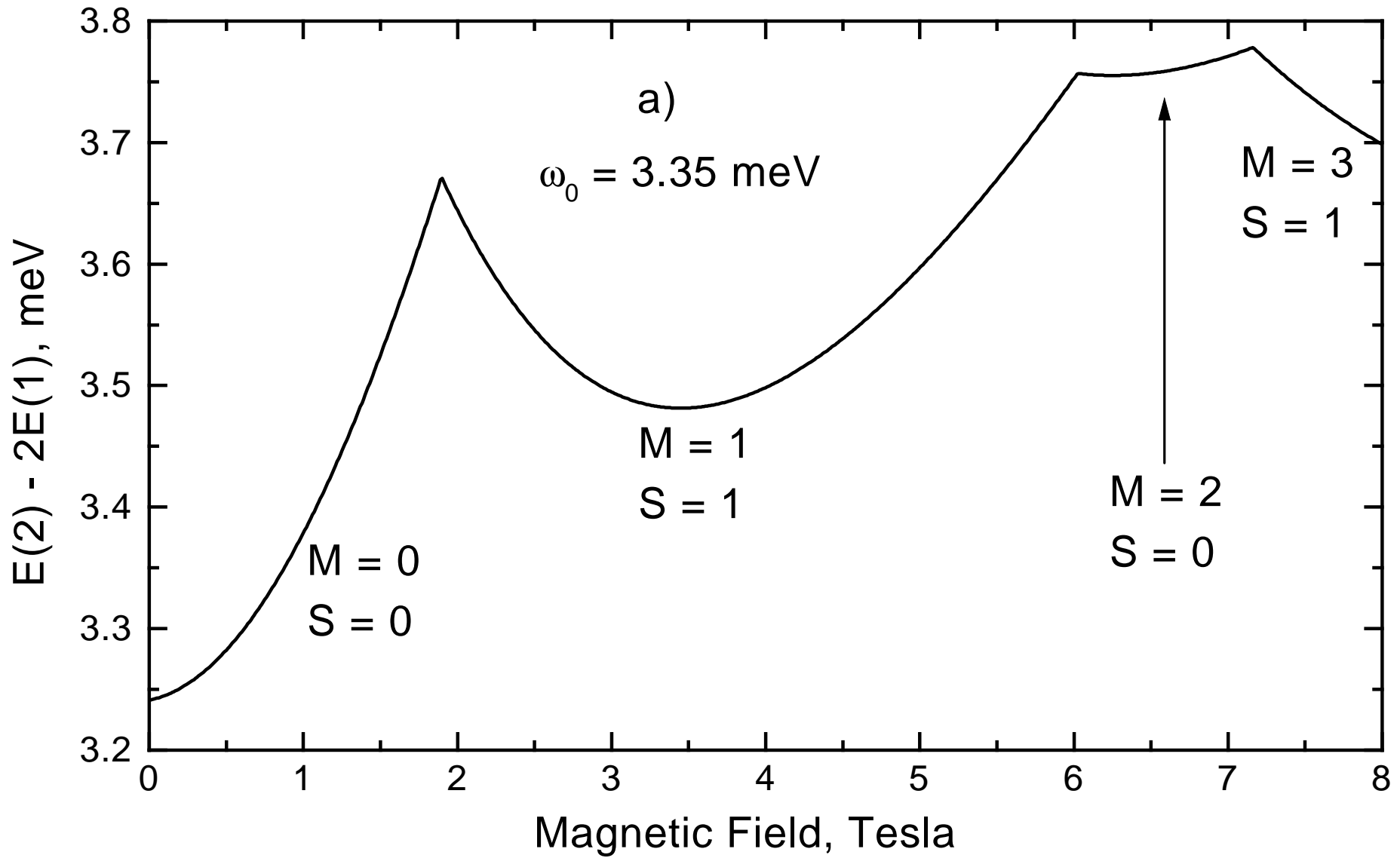


Fig. 7a (E. Anisimovas and A. Matulis "Energy Spectra ...

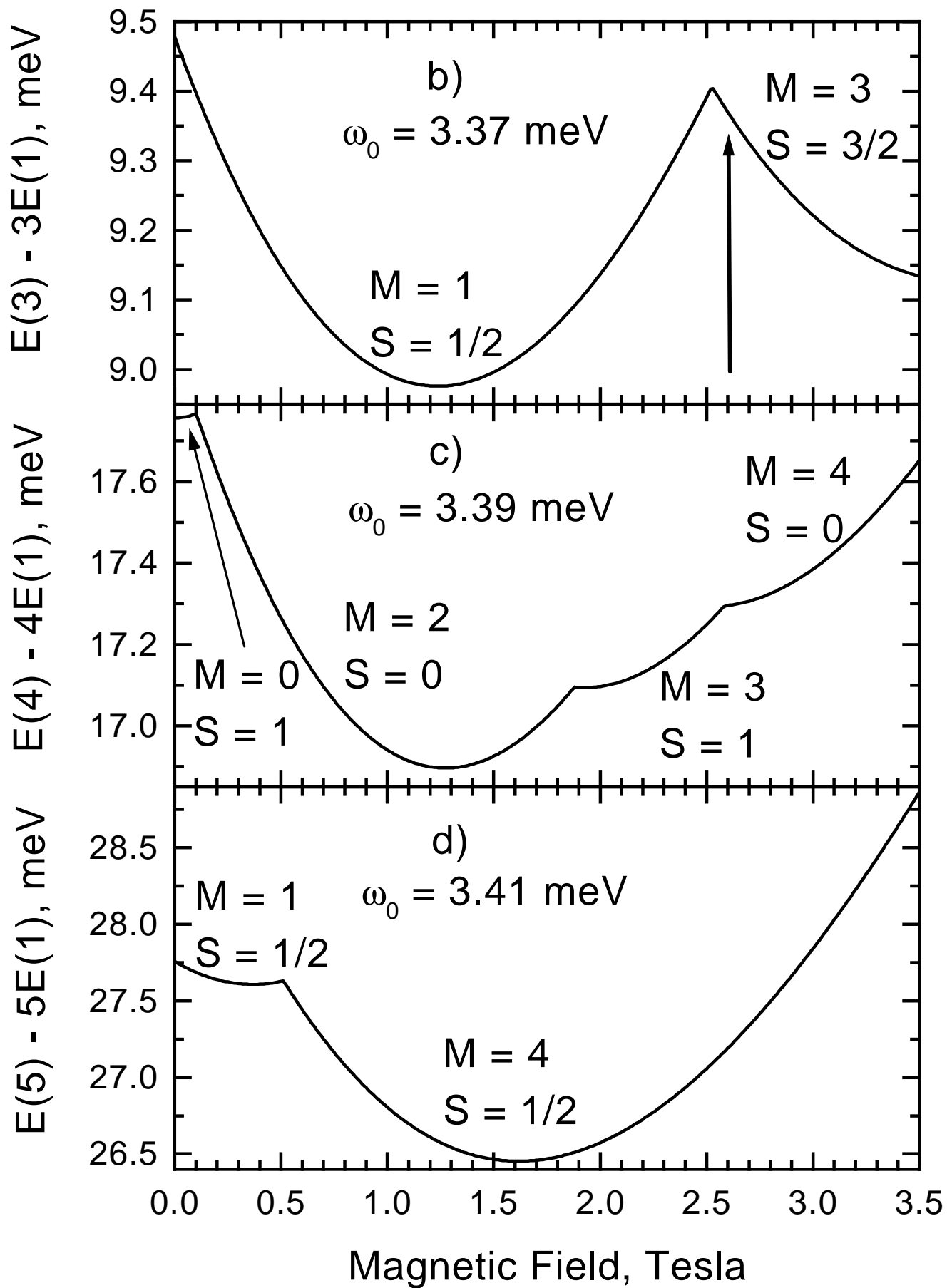


Fig. 7b-d (E. Anisimovas and A. Matulis "Energy Spectra ... ")